Photoreduction of CO_2 in an optical-fiber photoreactor: Effects of metals addition and catalyst carrier

The-Vinh Nguyen [1], Jeffrey C.S. Wu [*]

Department of Chemical Engineering, National Taiwan University, Taipei 10617, Taiwan

Abstract

The transformation of CO_2 to hydrocarbons using sunlight is one of best routes to produce renewable energy. Photocatalytic reduction of CO_2 with H_2O in the gaseous phase is studied by using Cu-Fe/TiO_2 catalyst coated on optical fibers under UVA and UVC irradiation. Catalyst coated optical fibers are assembled in the reactor such that the UV light can enter along the fibers to conduct the photocatalytic reaction on its surface. Methane and ethylene as main products are observed to evolve from this photoreactor. The presence of Fe as a co-dopant in Cu/TiO_2 catalyst is found to synergistically reduce CO_2 with H_2O to ethylene at the quantum yield and total energy efficiency of 0.024% and 0.016%, respectively. This phenomenon is well explained by an efficient charge transfer mechanism between TiO_2 as a support and Cu as well as Fe as co-dopants. Methane is formed more favorably than ethylene on Cu/TiO_2. Meanwhile, Fe as a co-dopant on Cu/TiO_2 catalyst is found to depress the methane formation. The photo production of ethylene over catalysts supported on optical fibers presents yields that are one order of magnitude higher than that on the glass plate counterpart. For a given amount of catalyst and light energy, the optical-fiber reactor can utilize light energy efficiently. Many photo-driven reactions will have advantage using such optical-fiber system.
© 2007 Elsevier B.V. All rights reserved.

Keywords: Photocatalytic reduction; Cu-Fe/TiO_2; Carbon dioxide; Charge transfer; Optical fiber

1. Introduction

Among the top 10 problems of humanity in the next 50 years, an energy crisis and environmental pollution come first and foremost on the list [1]. Although the price of fossil fuel is strongly dependent on the political status of the world, it has substantially increased over the years. In spite of this fact, consumption of fossil fuel dramatically increases worldwide year after year because of the strong demand for human activities. Meanwhile, carbon dioxide emissions mainly released by burning fossil fuels are the major cause of the global warming effect.

Solar energy is the Earth's ultimate energy supply. Inspired by the photosynthesis process of plants, algae and photosynthetic bacteria that use sunlight energy to drive the synthesis of organic compounds, a large number of research groups have been doing research on hydrocarbon production by employing CO_2 and H_2O with the helps of UV irradiation and photocatalysts [2–15]. Ruthenium bipyridine complexes as homogeneous catalysts or photosensitizers were reported to reduce CO_2-saturated DMF solution under visible light to formate at the average yield of 20–30 μmol/h [2,4]. Around one decade later, Heleg and Willner claimed to photocatalytically fix CO_2 to formate and H_2 under visible light in an aqueous system containing eosin-modified Pd-TiO_2 powder and sacrificial agents [5]. The formate production rate of this system was measured at ca. 1 μmol/h, which is five-fold higher than the Pd-TiO_2 counterpart [5]. Saji research group also reported the formation of acetaldehyde and alcohols, and gaseous products such as methane, ethane and ethylene as minor portions in the aqueous solution of TiO_2 powder mixed with CO_2 and NaOH under high pressure CO_2 gaseous phase [6]. Production rate of acetaldehyde was observed at around 1 μmol/g-cat h under UVC and 2.5 MPa of CO_2 gas [6]. Photoreduction of CO_2 using TiO_2 powder in liquid CO_2 under UVC was also reported by Saji's group with the production rate of formic acid of 0.28 μmol/g-cat h without any other gaseous products [7]. Guan et al. previously reported the photoreduction

of CO_2 over $K_2Ti_6O_{13}$ photocatalyst combined with Cu/ZnO catalyst in aqueous solution under both UVC and concentrated sunlight [10]. Much hydrogen (68 μmol/g-cat h) evolved on Pt-$K_2Ti_6O_{13}$ catalyst whereas ca. 3 μmol/g-cat h of formic acid was obtained on Pt-Cu/ZnO/$K_2Ti_6O_{13}$ catalyst under Hg-lamp [10]. Meanwhile, under concentrated sunlight with energy up to 5.32 kWh/m^2, Pt-$K_2Ti_6O_{13}$ catalyst was found by these authors to significantly produce H_2 (32.8 μmol/g-cat h), HCHO (5.6 μmol/g-cat h) and HCOOH (20.7 μmol/g-cat h) in comparison with Pt-Cu/ZnO/$K_2Ti_6O_{13}$ catalyst [10].

Recently in our group, Cu/TiO_2-based photocatalysts have been synthesized by sol–gel methods to reduce CO_2 to hydrocarbons in aqueous solution and gaseous phase [9,13–15]. In addition to the low quantum and energy efficiency of these photocatalysts towards CO_2 reduction, the liquid-phase photoreactor presents several drawbacks, such as low light-utilization efficiencies due to absorption and scattering of the light by the reaction medium and restricted processing capacities due to mass transport limitations.

The transmission and uniform distribution of light energy are important in designing a photoreactor which differs completely from a traditional reactor. Traditional packed-bed reactor with light irradiation either from side or center always projects shadow on the other side of catalyst particle. Thus certain percentage of photocatalyst surface cannot be photo-activated in a reaction. How to evenly deliver sufficient photons to the catalyst is a crucial factor in a photoreactor. In order to solve these problems, a novel system using optical fibers as a means of light transmission and distribution to solid-supported photocatalysts was first proposed by Marinangeli and Ollis [16,17]. Although the optical-fiber reactor systems used to be considered not practical owing to the heat buildup as well as the handling of extremely thin fiber, these problems are easily overcome nowadays [18]. A bundle of optical fibers provide a very high exposure surface. Optical fibers can be used to transmit the light uniformly inside the module of the photoreactor. This kind of design offers an economical way to deliver photons uniformly in a large volume, a step toward industrial large-scale photoreactor.

In this present study, in order to closely mimic the photosynthesis process of plants, we report as the first time the photoreduction of CO_2 to hydrocarbons in gaseous phase by using optical fibers coated with Cu-Fe/TiO_2 catalyst. The improvement of hydrocarbons production efficiency by using photo-reactor design approach as well as the reaction mechanism are also discussed.

2. Experimental

2.1. Catalyst preparation

Commercial titanium dioxide powder (P25, Degussa) was used as a TiO_2 source. $Cu(NO_3)_2 \cdot 3H_2O$ and $Fe(NO_3)_3 \cdot 9H_2O$ (Aldrich) were employed as precursors of metal dopants on TiO_2 support. The polymer clad of the optical fiber (ET tone Taiwan) was removed by calcination at 500 °C for 3 h. This step was followed by washing off the remaining residue with

10 M NaOH aqueous solution then distilled water in an ultrasonic bath three times.

For the preparation of metal supported TiO_2 thin-film, TiO_2 slurry with corresponding metal salts was prepared by the incremental addition of 2 ml of aqueous polyethylene glycol (Merck, average MW of 20,000) solution with metal salts to 0.5 g of TiO_2 powder in a mortar under vigorous grinding with pestle [19]. Each 0.1 ml of the aqueous polyethylene glycol solution was added after the previous mixture had formed a uniform and lump-free paste. Thereafter the prepared uniform slurry was coated on optical fibers by dip coating method or on glass plates by a doctor blade technique. After natural drying at room temperature, the thin film was calcined in static air at 450 °C for 30 min.

2.2. Characterization

TiO_2 thin films were characterized with X-ray diffraction (XRD, Phillips, Cu Kα radiation) for crystallinity, scanning electron microscopy with energy dispersive X-ray spectrometer (SEM-EDX, Philips XL30, EDAX DX4) for film thickness and surface morphology, nitrogen adsorption (Micromeritics ASAP 2000) for BET specific surface area, pore size and pore volume. The band-gap energies of TiO_2 films were determined by UV–vis diffuse reflectance spectroscopy (UV–vis DRS, Varian Cary 100). The light intensity was measured with a Lumen meter (Exfo). XPS measurements were taken on a VG Microtech MT500 spectrometer, operated with a constant pass energy of 50 eV and with Mg Kα radiation as the excitation source ($hv = 1253.6$ eV). The catalyst was pressed into a pellet, and then adhered on the sample holder by carbon tape. Carbon (1 s, 284.5 eV) was used as an internal standard for binding energy calibration.

Quantum yield (Φ) of the reaction is approximately calculated by using Eqs. (1) and (2). Eight or twelve electrons are required to transform CO_2 to methane or ethylene, respectively. Energy efficiency (η) is estimated by Eq. (3), which represents the conversion of photo to chemical energy.

$$\Phi_{CH_4}(\%) = \frac{[8 \times \text{moles of methane yield}] \times 100\%}{[\text{mole of photon absorbed by catalyst}]} \quad (1)$$

$$\Phi_{C_2H_4}(\%) = \frac{[12 \times \text{moles of methane yield}] \times 100\%}{[\text{mole of photon absorbed by catalyst}]} \quad (2)$$

$$\eta(\%) = \frac{\begin{array}{c}[\text{heat of combustion of methane (ethylene)} \\ \times \text{ mole of methane (ethylene) yield}] \times 100\%\end{array}}{[\text{energy of photon absorbed by catalyst}]} \quad (3)$$

where, heat of combustion of methane and ethylene are 802 and 1411 kJ/mole, respectively.

The mole of photon absorbed by catalyst was assumed to be equal to that absorbed by the number of optical fibers employed in the reactor. The latter value was estimated on the basis of the outlet energy subtracted from the inlet energy through the optical-fiber reactor [20]. In order to avoid the scattering of light out of the aperture of Lumen meter, the total number of optical fibers (typically 216) in the reactor were put in one

narrow Pyrex glass tube with a diameter of 5 mm and length same as that of the optical fibers (110 mm). A blank measurement of photon absorbed by the Pyrex glass tube without optical fibers was also measured to get the net value of photon absorbed by the number of optical fibers.

The amount of catalyst coated on carriers including glass plate and optical fiber is determined by the difference between the weight of catalyst coated carrier and that of bare carrier. Owing to the very small amount of catalyst coated on one optical fiber, the amount of catalyst coated on this carrier is measured on the basis of the total number of optical fibers in the photoreactor which is 117, 216 or 450 fibers.

2.3. Photocatalytic conversion of CO_2

Photocatalytic reaction was carried out in a continuous circular Pyrex glass reactor (216 cm^3) with a quartz window for conduction of light irradiation. Catalyst coated optical fibers were assembled in the reactor such that the light source (high pressure Hg lamp, 150 W) can enter along the fibers to conduct the photocatalytic reaction on its surface as shown in Fig. 1(a) [15]. The UVA (320–500 nm) and UVC (250–450 nm) light for different reactions were obtained by using appropriate color filters (Exfo). The light intensity was measured on the quartz window with unit of mW/cm^2. The

reactor was covered with a heating tape connected to a temperature controller with a thermocouple placed at the top of the catalyst bed to maintain the reaction at around 75 °C. The reactor was purged by CO_2 gas bubbling through distilled water for 1 h at 75 °C before and during the reaction. The space velocity of CO_2 gas and H_2O vapor was maintained at 0.72 h^{-1} for every experiment. The outlet gases were analyzed at certain periods of time by using GC equipped with FID and porapak Q column.

The increase of the number of optical fibers used in the same photoreactor, which does not significantly affect the flow of reactants as well as the diffusion of products from the optical-fiber surface to the gas flow, was done with care to ensure that the fibers are separate from one another. For comparison, the photocatalytic conversion of CO_2 into hydrocarbons on glass plates coated with catalysts was also studied.

3. Results

3.1. Catalyst characterization

The specific surface area and band-gap energy of various catalysts are shown in Table 1. As TiO_2 is loaded with 1 wt% of Cu and Fe, its specific surface area is slightly decreased from 50.00 to 47.74 m^2/g. Band-gap energy of Cu (1 wt%)-Fe
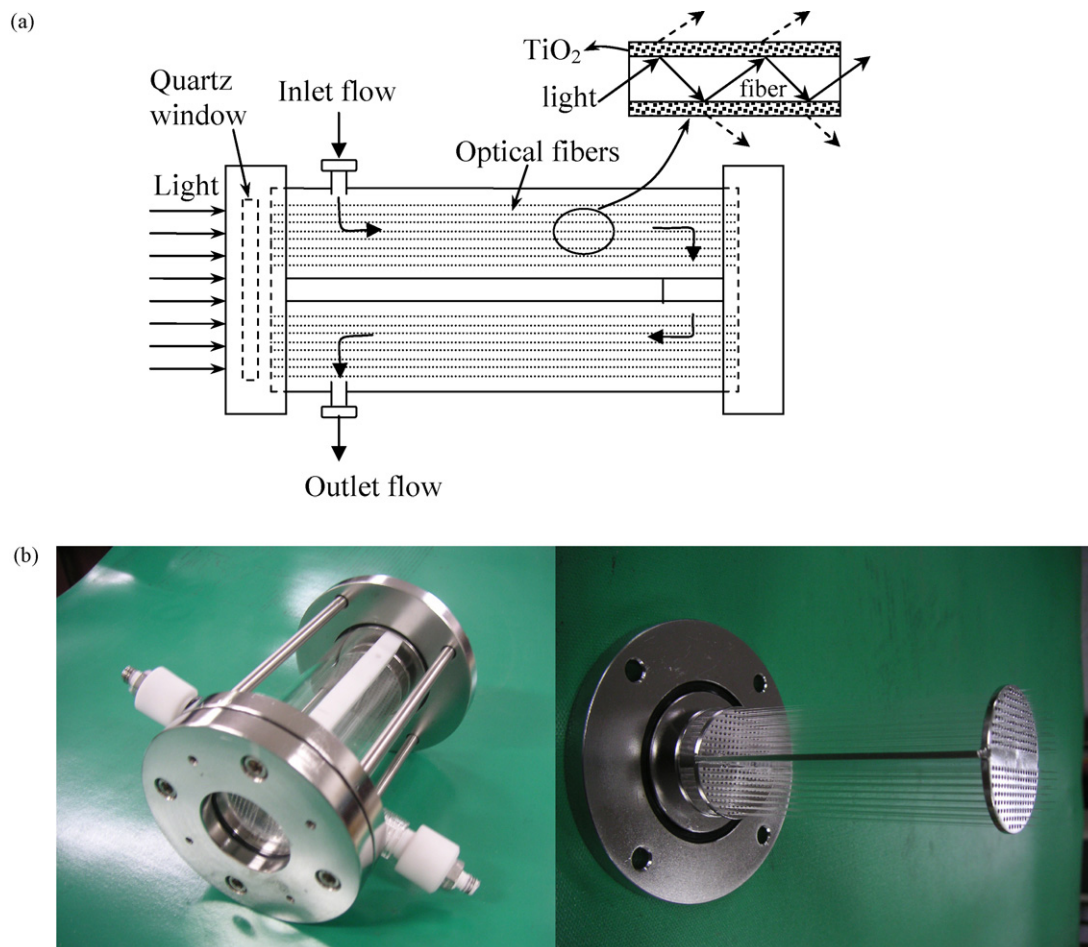

Fig. 1. Schematic diagram (a) and images (b) of photoreactor with catalyst coated optical fibers.

Table 1
Specific surface area and band-gap energy of various catalysts

Photocatalyst	S_{BET} (m^2/g)	E_g (eV)
TiO$_2$-P25	50.00	3.11
Cu(1 wt%)/TiO$_2$	–	3.09
Fe(1 wt%)/TiO$_2$	–	3.00
Cu(1 wt%)-Fe(1 wt%)/TiO$_2$	47.74	2.93

(1 wt%)/TiO$_2$ (2.93 eV) is also observed to decrease in comparison with that of bare TiO$_2$ (3.11 eV).

Fig. 2 depicts the SEM images of metal loaded TiO$_2$ films coated on glass plate and optical fiber. The thickness of the thin films on glass plate and optical fiber are around 12 μm and 878 nm, respectively. Some cracks are observed on the morphological surface of the TiO$_2$ thin film coated on glass plate. Meanwhile, continuous and uniform thin film of TiO$_2$ is obtained when coated on optical fiber. This difference is probably due to the thickness of the former is much higher than that of the latter.

X-ray diffraction patterns of different catalysts coated as thin films on glass plates are shown in Fig. 3. There is no difference between the X-ray diffraction pattern of bare TiO$_2$ and that of metal loaded TiO$_2$. The result implies that Cu and Fe are well dispersed on the surface of the TiO$_2$ support.

In order to elucidate the UV and visible light absorption of metal loaded TiO$_2$ films, UV–vis diffuse reflectance spectroscopy of different catalysts are measured and depicted in Fig. 4. Cu as a dopant on TiO$_2$ does not significantly affect the light absorption property of bare TiO$_2$ film as shown in Fig. 4b. Nevertheless, when Fe is supported on TiO$_2$ either with or without Cu as a co-dopant, the derived catalysts appear to
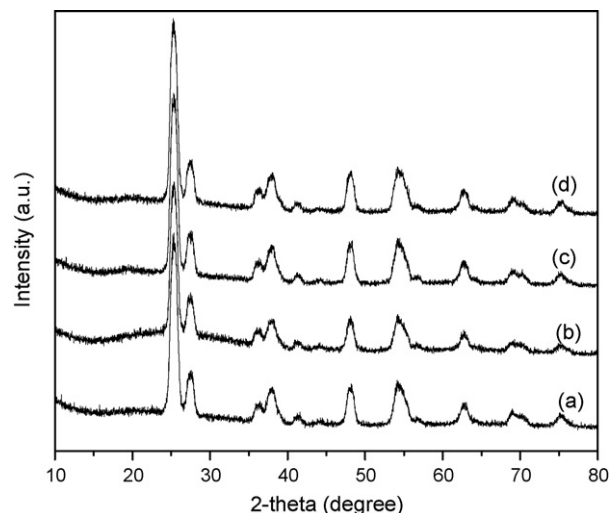

Fig. 3. X-ray diffraction patterns of different catalysts. (a) TiO$_2$-P25, (b) Cu(1 wt%)/TiO$_2$, (c) Fe(1 wt%)/TiO$_2$ and (d) Cu(1 wt%)-Fe(1 wt%)/TiO$_2$.

absorb visible light with a small peak at around 500 nm of wavelength (Fig. 4c and d). This result could be due to the visible light absorption of iron oxides with band-gap energies of 2.0–2.3 eV [21].

Fig. 5 depicts the XPS spectra of Cu(0.5 wt%)-Fe(0.5 wt%)/TiO$_2$ catalyst. The binding energies of Cu 2p$_{3/2}$ and 2p$_{1/2}$ are 931.9 and 951.2 eV, respectively (Fig. 5a), which could be assigned to Cu$_2$O compound on the surface of TiO$_2$ [22]. Meanwhile, Fig. 5b shows that the binding energies of Fe 2p$_{3/2}$ and 2p$_{1/2}$ are 710.3 and 725.1 eV, respectively. These binding energies correspond to Fe$_2$O$_3$ compound on the surface of TiO$_2$ [22].
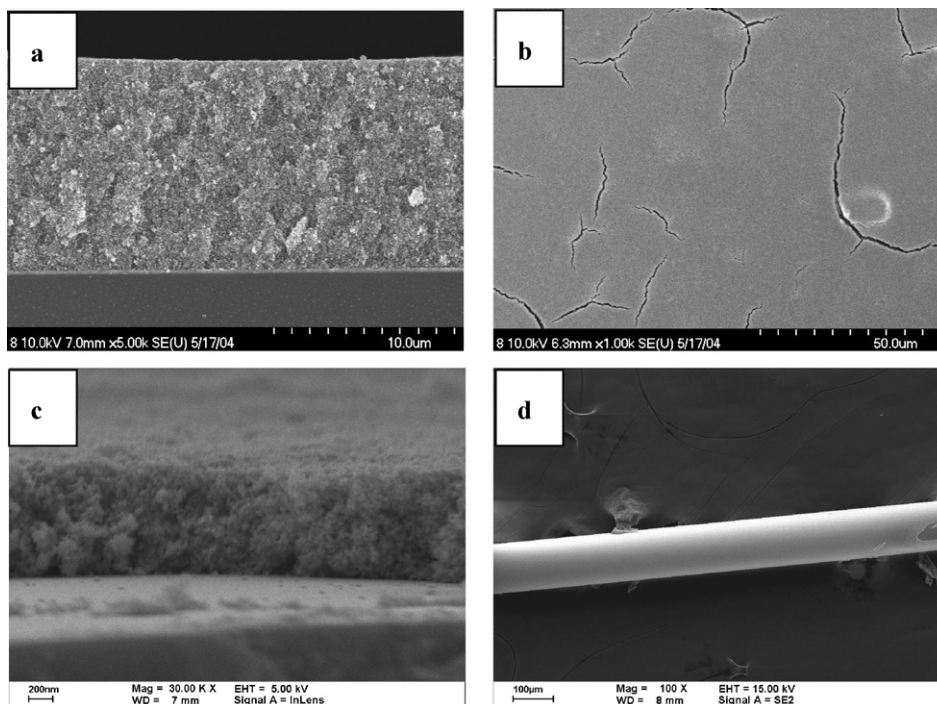

Fig. 2. SEM images of TiO$_2$ film coated on glass plate (a and b) and on optical fiber (c and d). (a and c) Cross-section and (b and d) surface morphology view.
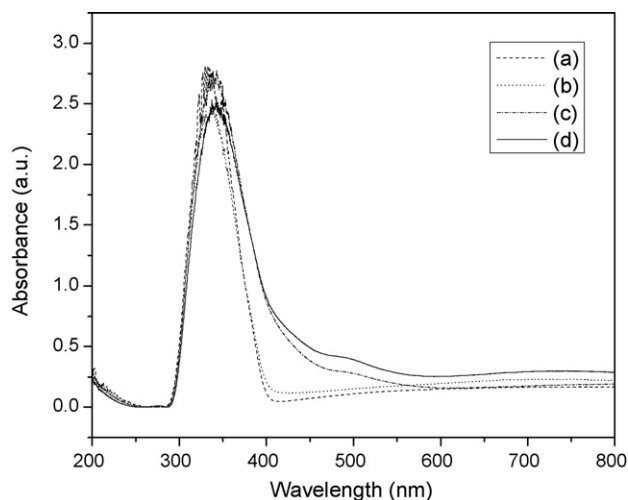
Fig. 4. UV–vis spectroscopy of different catalysts. (a) TiO$_2$-P25, (b) Cu(1 wt%)/TiO$_2$, (c) Fe(1 wt%)/TiO$_2$ and (d) Cu(1 wt%)-Fe(1 wt%)/TiO$_2$.

3.2. Photocatalytic conversion of CO_2 into hydrocarbons

In this study, Cu-Fe/TiO$_2$ catalysts are observed to photoreduce CO_2 with H$_2$O to various kinds of products that
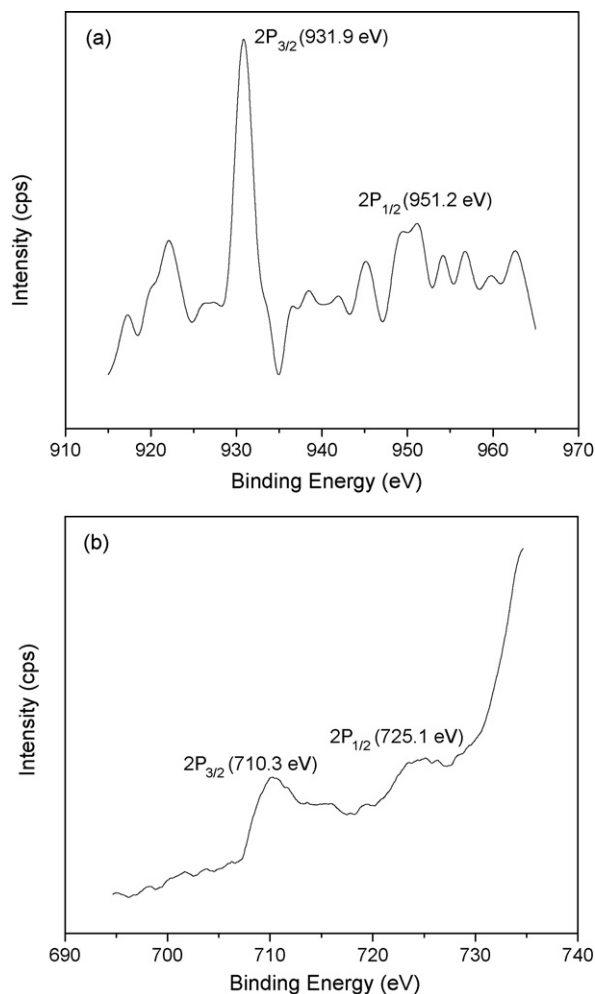
Fig. 5. XPS spectroscopy of Cu(0.5wt%)-Fe(0.5wt%)/TiO$_2$ catalyst. (a) XPS spectrum of Cu2p and (b) XPS spectrum of Fe2p.
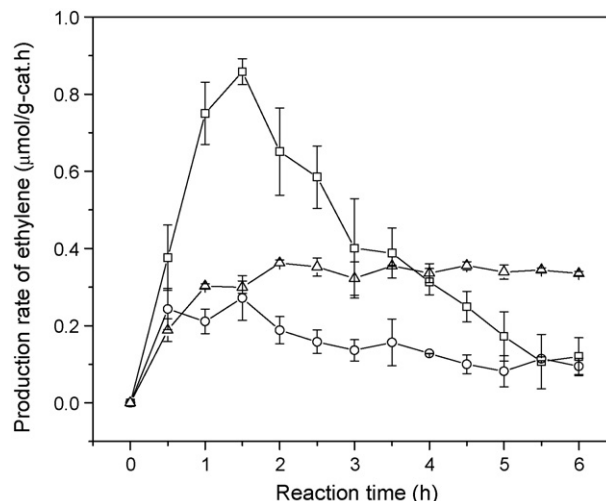

Fig. 6. Production rate of ethylene over various kinds of photocatalysts according to reaction time. (□) Cu(1 wt%)/TiO$_2$, (○) Fe(1 wt%)/TiO$_2$, (△) Cu(1 wt%)-Fe(1 wt%)/TiO$_2$. The irradiation source was in UVC range (250–450 nm) with the intensity of 225 mW/cm^2. Photocatalysts were coated on 216 optical fibers.

include significant amounts of ethylene and methane as well as trace amounts of ethane and methanol. The production rate of ethylene over different catalysts coated on optical fibers according to reaction time is presented in Fig. 6. According to the results, the production rate of main products including methane and ethylene over most catalysts, especially Cu-Fe/TiO$_2$, under different reaction conditions reaches to steady-state at around 4 h after turning on the light source. Consequently, the production rate of main products is determined on the basis of average production rate after a reaction time of 4 h.

Table 2 presents the production rate of ethylene over different photocatalysts and carriers under UVC (250–450 nm). TiO$_2$ shows negligible photocatalytic activity towards ethylene production. When either Cu or Fe is loaded on the TiO$_2$ support, the derived catalysts appear to reduce CO_2 with H$_2$O to ethylene. Moreover, as Cu and Fe are employed as co-dopants on the TiO$_2$ support, the resulting Cu-Fe/TiO$_2$ catalyst performs the synergistic effect in terms of CO_2 photoreduction to

Table 2
Production rate of ethylene over different photocatalysts and carriers under UVC

Photocatalyst	Ethylene production rate over glass plate (μmol/g h)[a]	Ethylene production rate over optical fiber (μmol/g h)[a]
TiO$_2$-P25	0.00	0.00
Cu(1 wt%)/TiO$_2$	0.01	0.24
Fe(1 wt%)/TiO$_2$	0.02	0.08
Cu(1 wt%)-Fe(1 wt%)/TiO$_2$	0.04	0.35
Cu(0.5 wt%)-Fe(0.5 wt%)/TiO$_2$	0.05	0.58
Cu(0.25 wt%)-Fe(0.25 wt%)/TiO$_2$	0.03	0.53

[a] Ethylene production rate was determined on the basis of average production rate after the reaction time of 4 h. The irradiation source was in UVC range (250–450 nm) with the intensity of 225 mW/cm^2.

Table 3
Production rate of ethylene and methane over different photocatalysts under UVA

Photocatalyst	Ethylene production rate over glass plate (μmol/g h)[a]	Methane production rate over glass plate (μmol/g h)[a]
TiO_2-P25	0.00	Trace
Cu(1 wt%)/TiO_2	0.01	0.09
Fe(1 wt%)/TiO_2	0.02	0.06
Cu(1 wt%)-Fe(1 wt%)/TiO_2	0.04	0.06
Cu(0.5 wt%)-Fe(0.5 wt%)/TiO_2	0.05	0.06
Cu(0.25 wt%)-Fe(0.25 wt%)/TiO_2	0.01	0.19

[a] Methane and ethylene production rate were determined on the basis of average production rate after the reaction time of 4h. The irradiation source was in UVA range (320–500 nm) with the intensity of 225 mW/cm^2.

Table 4
Effect of carrier on production rate of ethylene and methane under UVA

Photocatalyst	Ethylene production rate (μmol/g h)[a]	Methane production rate (μmol/g h)[a]
Cu(0.5 wt%)-Fe(0.5 wt%)/TiO_2/glass plate	0.05	0.06
Cu(0.5 wt%)-Fe(0.5 wt%)/TiO_2/optical fiber	0.58	0.91

[a] Methane and ethylene production rate were determined on the basis of average production rate after the reaction time of 4 h. The irradiation source was in UVA range (320–500 nm) with the intensity of 225 mW/cm^2.

ethylene. The optimum amount of Cu and Fe loading on TiO_2 are determined to be 0.5 wt% for each with the corresponding amount of evolved ethylene at 0.58 μmol/g-cat h as shown in Table 2. The production rate of ethylene, based on per gram catalyst, on optical fibers is found to be one order of magnitude higher than that on glass plate.

Production rate of ethylene and methane over different photocatalysts under UVA are shown in Table 3. According to the results in Tables 2 and 3, the light source does not substantially affect the production rate of ethylene over the catalyst coated on glass plate. The maximum amount of ethylene at 0.05 μmol/g-cat h is observed on the Cu(0.5 wt%)-Fe(0.5 wt%)/TiO_2 coated glass plate, which is similar to that under UVC irradiation. Meanwhile, methane production rate over different catalysts presents different trends. The highest amount of methane at 0.19 μmol/g-cat h is measured on Cu(0.25 wt%)-Fe(0.25 wt%)/ TiO_2, whereas methane production rate of ca. 0.06 μmol/g-cat h is observed on Fe(1 wt%)/TiO_2, Cu(1 wt%)-Fe(1 wt%)/TiO_2 and Cu(0.5 wt%)-Fe(0.5 wt%)/TiO_2 catalysts.

Production rate of ethylene and methane on Cu(0.5 wt%)-Fe(0.5 wt%)/TiO_2 catalyst under UVA on different carriers are shown in Table 4 for comparison. It is interesting that under UVA irradiation, catalysts supported on optical fibers also produces an amount of ethylene one order of magnitude higher than that on glass plate. Moreover, the amount of produced

methane on catalysts supported optical fibers is 15 times higher than that on its glass plate counter part.

Quantum yields of ethylene and methane production over different catalysts are presented in Tables 5 and 6. The quantum yield under UVA is one order of magnitude higher than that under UVC. Because quantum yield is inversely proportional to molar quantity of photons absorbed on catalysts as shown in Eqs. (1) and (2), it is also inversely proportional to the photon energy absorbed by optical fibers. The optical fibers used in this study are made of quartz glass, which show on absorption of UVC light (280×10^{-3} J s^{-1} per 216 fibers) stronger than that of its UVA counterpart (17.4×10^{-3} J s^{-1} per 216 fibers). Consequently, the quantum yield under UVC is much lower than that under UVA owing to the wasted photons absorbed by optical fibers due to heat.

The quantum yields of ethylene and methane production on Cu(0.5 wt%)-Fe(0.5 wt%)/TiO_2 catalyst under UVA are found to be similar at values of 0.024 and 0.025, respectively. The data of quantum yields under UVA are comparable to those reported by Aurian-Blajeni et al. for photoreduction of CO_2 in aqueous solution [23]. However, the data of quantum yields under UVC are one order of magnitude higher than those reported by Hofstadler et al. for UVC photominerallization of 4-Chlorophenol using TiO_2 immobilized on fused-silica glass fibers [24].

Table 5
Quantum yield (Φ) and energy efficiency (η) of ethylene and methane production over Cu(0.5 wt%)-Fe(0.5 wt%)/TiO_2/optical fiber under UVA

Photocatalyst	C_2H_4 evolution		CH_4 evolution	
	Φ (%)[a]	η (%)[a]	Φ (%)[a]	η (%)[a]
Cu(0.5 wt%)-Fe(0.5 wt%)/TiO_2/optical fiber	0.024	0.008	0.025	0.008

[a] One photon energy at 365 nm is 5.45×10^{-19} J. Photon energy absorbed by fibers is 17.4 mW (17.4×10^{-3} J s^{-1}). Total numbers of absorbed photon per second are 3.19×10^{16}.

Table 6
Quantum yield and energy efficiency of ethylene production over different photocatalysts coated on optical fibers under UVC

	Φ (%)[a]	η (%)[a]
TiO_2-P25	0	0
Cu(1 wt%)/TiO_2	0.00074	0.00022
Fe(1 wt%)/TiO_2	0.00026	0.00008
Cu(1 wt%)-Fe(1 wt%)/TiO_2	0.00108	0.00032
Cu(0.5 wt%)-Fe(0.5 wt%)/TiO_2	0.00178	0.00052
Cu(0.25 wt%)-Fe(0.25 wt%)/TiO_2	0.00162	0.00048

[a] One photon energy at 300 nm is 6.63×10^{-19} J. Photon energy absorbed by fibers is 280 mW (280×10^{-3} J s^{-1}). Total numbers of absorbed photon per second are 4.22×10^{17}.

Table 7 presents the comparison between ethylene production rate over Cu(0.5 wt%)-Fe(0.5 wt%)/TiO_2 photocatalysts under UVC and UVA irradiation. The production rate of ethylene on this catalyst is comparable under both UVC and UVA. The same result is also observed on two kinds of carriers, glass plate and optical fiber.

The effect of the number of optical fibers on the production rate of ethylene over Cu(1 wt%)-Fe(1 wt%)/TiO_2 photocatalyst is depicted in Table 8. The higher the number of optical fibers in the same volume of photoreactor as well as the same light irradiation condition, the larger the production rate of ethylene obtained.

4. Discussion

It was interestingly to find that either Cu or Fe alone as a dopant on TiO_2 catalyst shows a fast decline of photoreduction of CO_2 to ethylene as shown in Fig. 6. Cu(1 wt%)/TiO_2 strongly reduces CO_2 at the initial 2 h of reaction and significantly decreases its activity thereafter. Meanwhile, Fe(1 wt%)/TiO_2 shows relatively low photoactivity and its deactivation is also observed after 2 h of the reaction. There are a large number of previous reports about the electrochemical reduction of CO_2 at copper electrode [25–29], which present the selective formation of methane and ethylene as final products of this reaction. On the other hand, Fe metal electrode in aqueous hydrogen carbonate solution was found to only slightly produce methane [25]. Accordingly, the data in this present study imply to some extent that the photocatalytic and electrocatalytic activities of copper compounds are consistent with one another in terms of CO_2 reduction with H_2O to ethylene. Nevertheless, owing to the

Table 7
Production rate of ethylene over Cu(0.5 wt%)-Fe(0.5 wt%)/TiO_2 photocatalysts under UVC and UVA irradiation

Irradiation source	Ethylene production rate over glass plate (nmol/g h)[a]	Ethylene production rate over optical fiber (nmol/g h)[a]
UVC light (250–450 nm)	0.05	0.58
UVA light (320–500 nm)	0.05	0.58

[a] Ethylene production rate was determined on the basis of average production rate after the reaction time of 4h. The intensity of irradiation source was 225 mW/cm^2.

Table 8
Production rate of ethylene over Cu(1 wt%)-Fe(1 wt%)/TiO_2 photocatalyst according to the number of optical fiber

Number of optical fiber	Ethylene production rate (μmol/g h)[a]
117	0.28
216	0.35
450	0.57

[a] Ethylene production rate was determined on the basis of average production rate after the reaction time of 4 h. The irradiation source was in UVC range (250–450 nm) with the intensity of 225 mW/cm^2.

lack of an efficient "anode" to oxidize H_2O, the photocatalytic activity of Cu(1 wt%)/TiO_2 catalyst becomes significantly depressed because of charge recombination as shown in Fig. 6.

As Fe is a transition metal that has a set of consecutive oxidation states, typically Fe^{2+}/Fe^{3+}, the deliberate employment of Fe as a co-dopant on Cu/TiO_2 catalyst in this study could be a good process to shuttle the holes from TiO_2 to H_2O. Consequently, photocatalytic activity and stability of Cu-Fe/TiO_2 are much superior than those of Cu/TiO_2 and Fe/TiO_2 as presented in Table 2 and Fig. 6. Additionally, iron oxide is also well known as a good photocatalyst in terms of visible light absorption [21], which is well supported by the UV–vis DRS spectroscopy in Fig. 4. As a result, the photocatalytic activities of Cu-Fe/TiO_2 catalyst are observed to be comparable under UVA and UVC irradiation (Table 7).

It has been reported that the conduction band of iron oxide by Mott-Schottky measurements is slightly above [30,31] and below [32,33] the H^+/H_2 half-cell potential. The former claims were later confirmed by the report of Somorjai and Damme [21] who measured the flat-band potential of iron oxide varying between -0.9 and -1.1 V (vs. SCE) at pH 13. This value was well supported by the photocatalytic activity of iron oxide to decompose water to hydrogen [21]. Based on the flat-band potential of -1.1 V (vs. SCE) and band-gap energy of 2.2 eV of iron oxide [21] along with the band edge structure of TiO_2 [34,35] and redox potential of CO_2/C_2H_4 [29], the synergistic performance of Cu-Fe/TiO_2 catalyst towards photocatalytic reduction of CO_2 to ethylene could be well explained by the charge transfer mechanism as depicted in Fig. 7. The difference
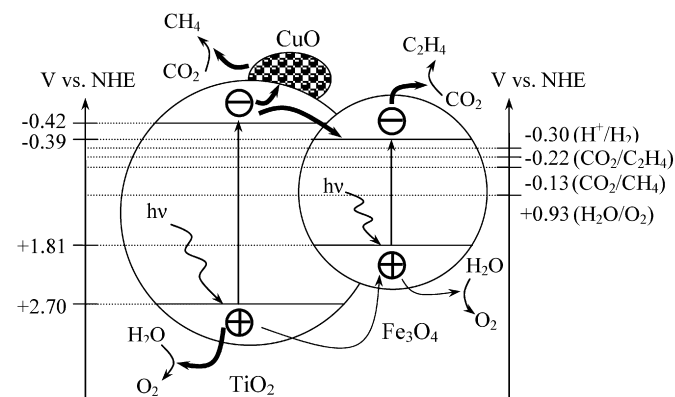

Fig. 7. Schematic illustration of band edge and charge transfer on Cu-Fe/TiO_2 at pH 5. The thick arrows represent the dominant pathways for hydrogen and oxygen evolution.

of flat-band potential between TiO_2, -0.42 eV, and iron oxide, -0.39 eV, causes the effective charge separation and the improved photoproduction of ethylene. Since the flat-band potential and valence band of iron oxide are lower and higher than those of TiO_2, respectively, photo-excited electrons and holes would tend to recombine easily provided that the transfer speeds of electrons and holes from TiO_2 to iron oxide were almost the same. However, the cooperative motion of the holes is an inherently slower process than that of electrons, which is ascribed to the much higher mobility of the latter than the former [36]. As a result, the electrons transferred from TiO_2 to iron oxide or copper oxide easily reduce CO_2 to produce ethylene before they recombine with the holes which are moving from TiO_2 to iron oxide or directly taking part in the oxygen formation reaction on the TiO_2 surface. Accordingly, the effective reduction of CO_2 for the production of ethylene is taken place by the electron moved from TiO_2 to iron oxide and to copper oxide. Meanwhile, oxygen seems to be mainly evolved by the holes on TiO_2 itself rather than the holes transferred from TiO_2 to iron oxide, resulting in the improvement of photocatalytic performance due to the reverse flows of electrons and holes as shown in Fig. 7. This phenomenon was also observed in the previous study for the RuS_2/TiO_2-SiO_2 catalyst in the reaction of photocatalytic decomposition of water to hydrogen [35].

The data in Table 3 for methane production infer that the presence of Fe in Cu/TiO_2 catalyst seems to depress the evolution of methane. It was well known that the electrochemical reduction of CO_2 on single crystal copper electrodes formed various kinds of hydrocarbon products depending on its index planes [28,37,38]. Ethylene was formed more favorably than methane on the (1 0 0) electrode whereas methane was predominantly produced on the (1 1 1) surface [38]. Cu/TiO_2 in this present study favorably produces methane rather than ethylene, which implies that Cu as a dopant on TiO_2 catalyst might be in the form of (1 1 1) surface to some extent. Meanwhile, Fe/TiO_2 shows relatively low photoactivity to produce methane as compared to the Cu counterpart, which is consistent with a previous study [25]. Although Fe as a co-dopant on Cu/TiO_2 catalyst is observed to give rise to the synergistic performance of CO_2 reduction to ethylene, it substantially decreases the photoactivity towards methane production. High dispersion of metal dopants on supports was widely agreed to enhance the activities of derived catalysts [21]. Accordingly, the presence of Fe on Cu/TiO_2 somehow decreases the high dispersion of Cu on TiO_2 resulting in the decline of methane evolution on Cu-Fe/TiO_2 catalyst. This explanation could be supported by the result that the production rate of methane on Cu(0.25 wt%)-Fe(0.25 wt%)/TiO_2 is higher than those on Cu(0.5 wt%)-Fe(0.5 wt%)/TiO_2 and Cu(1 wt%)-Fe(1 wt%)/TiO_2. Owing to the synergistic effect towards ethylene production by using Cu and Fe as co-dopants on the TiO_2 catalyst, the increasing in metal loadings on TiO_2 catalyst that result in their low dispersion on the support could be compensated by the efficient charge transfer mechanism. Consequently, maximum production rate of ethylene is measured on Cu(0.5 wt%)-Fe(0.5 wt%)/TiO_2 with 0.05 and

0.58 μmol/g-cat·h for glass plate and optical fiber as carriers, respectively.

The effect of the number of optical fibers on ethylene production of Cu-Fe/TiO_2 catalyst gives the interesting results shown in Table 8. The more fibers assembled in the reactor, the higher the production rate of ethylene (based per gram catalyst) is measured under the same reaction conditions. The weight of catalyst coated on 117, 216 and 450 optical fibers are 3.5, 6.4 and 13.3 mg, respectively. Accordingly, the higher the amount of catalyst employed in the photoreactor, the higher the production rate of ethylene. In other words, these results imply that the light energy is over supplied in the photoreduction system. Otherwise, the production rate of ethylene could be observed to decrease. There might exist an optimum light intensity to give a maximum quantum yield for a given amount of catalyst in the photoreactor, in which the light energy can be completely utilized. This explanation is well supported by the comparison between the production rate of ethylene over the same catalyst coated on glass plate and optical fiber in Table 7. 72.0 and 6.4 mg of catalyst are measured on the former and latter, respectively. The amount of catalyst coated on glass plate is much higher than that of the optimum value, resulting in the depressed ethylene production rate (on a catalyst weight basis). Meanwhile, 6.4 mg of catalyst coated on 216 optical fibers is not sufficient to give a maximum quantum yield in this photoreduction system. Conclusively, for a given amount of catalyst and light energy, the optical fiber photoreactor is found to be over supplied with light irradiation in our current system, whereas the glass plate counterpart lacks photon adsorption on the catalyst, which gives rise to the superior photoproduction of the former system. Therefore, a higher production rate is expected if more optical fibers can be packed in the current reactor volume. On the other hand, the quantum yield can be increased in our system when less light intensity is supplied.

5. Conclusions

Photoreduction of CO_2 with H_2O in gaseous phase to methane and ethylene by using optical fibers coated with Cu-Fe/TiO_2 catalyst is reported as the first time in this present study. Optical fiber as a catalyst carrier is found to significantly improve the production rate of ethylene with one order of magnitude higher than that on the glass plate counterpart. Synergistic performance of Cu-Fe/TiO_2 as compared to Cu/TiO_2 and Fe/TiO_2 catalysts is observed in terms of ethylene production at the quantum yield and total energy efficiency of 0.024% and 0.016%, respectively. This result could be ascribed to the efficient charge transfer mechanism between TiO_2 as a support and Cu as well as Fe as co-dopants. Methane is formed more favorably than ethylene on Cu/TiO_2. Meanwhile, Fe as a co-dopant is found to depress the photoproduction of methane. A rising photo production rate is found by increasing the number of optical fibers under the same light intensity indicating that either the light irradiation is over supplied or more optical fibers can be inserted in the current reactor volume. Light energy can be completely utilized to achieve higher quantum yields with an optimum design. In addition, a

higher processing capacity is possible because photocatalyst can be coated on a large external area of optical fibers in a given reactor volume. Therefore, such optical-fiber reactor with commercial scale can be applied to many photoreactions, such as wastewater degradation or bioreactor either in vapor or liquid phase.

Acknowledgements

References

[1] R. Smalley, Energy & Nanotechnology Conference, Rice University, Houston, USA, May 3, 2003.
[2] J. Hawecker, J.-M. Lehn, R. Ziessel, J. Chem. Soc., Chem. Commun. (1985) 56.
[3] K. Thampi, J. Kiwi, M. Grätzel, Nature 327 (1987) 506.
[4] H. Ishida, K. Tanaka, T. Tanaka, Chem. Lett. (1987) 1035.
[5] V. Heleg, I. Willner, J. Chem. Soc., Chem. Commun. (1994) 2113.
[6] T. Mizuno, K. Adachi, K. Ohta, A. Saji, J. Photochem. Photobiol. A: Chem. 98 (1996) 87.
[7] S. Kaneco, H. Kurimoto, K. Ohta, T. Mizuno, A. Saji, J. Photochem. Photobiol. A: Chem. 109 (1997) 59.
[8] H. Yoneyama, Catal. Today 39 (1997) 169.
[9] I.-H. Tseng, W.-C. Chang, J.C.S. Wu, Appl. Catal. B: Environ. 37 (2002) 37.
[10] G. Guan, T. Kida, T. Harada, M. Isayama, A. Yoshida, Appl. Catal. A: Gen. 249 (2003) 11.
[11] Y. Shioya, K. Ikeue, M. Ogawa, M. Anpo, Appl. Catal. A: Gen. 254 (2003) 251.
[12] G. Guan, T. Kida, A. Yoshida, Appl. Catal. B: Environ. 41 (2003) 387.
[13] I.-H. Tseng, J.C.S. Wu, H.-Y. Chou, J. Catal. 221 (2004) 432.
[14] I.-H. Tseng, J.C.S. Wu, Catal. Today 97 (2004) 113.
[15] J.C.S. Wu, H.-M. Lin, C.-L. Lai, Appl. Catal. A: Gen. 296 (2005) 194.
[16] R.E. Marinangeli, D.F. Ollis, AIChE 23 (1977) 415.
[17] R.E. Marinangeli, D.F. Ollis, AIChE 26 (1980) 1000.
[18] W. Wang, Y. Ku, Chemosphere 50 (2003) 999.
[19] T.-V. Nguyen, H.-C. Lee, O.-B. Yang, Sol. Energy Mater. Sol Cells 90 (2006) 967.
[20] A. Danion, J. Disdier, C. Guillard, F. Abdelmalek, N. Jaffrezic-Renault, Appl. Catal. B: Environ. 52 (2004) 213.
[21] H.V. Damme, G.A. Somorjai, in: N. Serpone, E. Pelizzetti (Eds.), Photocatalyst-Fundamentals and Applications, John Wiley & Sons Press, New York, 1989, pp. 176, 299, 305.
[22] C.D. Wagner, W.M. Riggs, L.E. Davis, J.F. Moulder, G.E. Muilenberg, Handbook of X-ray Photoelectron Spectroscopy, Perkin-Elmer Corporation Press, 1978, pp. 76, 82.
[23] B. Aurian-Blajeni, M. Halmann, J. Manassen, Sol. Energy 25 (1980) 165.
[24] K. Hofstadler, R. Bauer, S. Novalic, G. Helsler, Environ. Sci. Technol. 28 (1994) 670.
[25] Y. Hori, K. Kikuchi, S. Suzuki, Chem. Lett. (1985) 1695.
[26] Y. Hori, A. Murata, R. Takahashi, S. Suzuki, J. Am. Chem. Soc. 109 (1987) 5022.
[27] Y. Hori, A. Murata, Y. Yoshinami, J. Chem. Soc. Faraday Trans. 87 (1991) 125.
[28] Y. Hori, I. Takahashi, O. Koga, N. Hoshi, J. Phys. Chem. B 106 (2002) 15.
[29] M. Gattrel, N. Gupta, A. Co, J. Electroanal. Chem. 594 (2006) 1.
[30] J.H. Kennendy, K.W. Frese, Fr., J. Electrochem. Soc. 125 (1978) 723.
[31] G. Horowitz, J. Eletroanal. Chem. 159 (1983) 421.
[32] J.S. Curran, W. Gissler, J. Electrochem. Soc. 126 (1979) 56.
[33] M. Anderman, J.H. Kennedy, J. Electrochem. Soc. 131 (1984) 21.
[34] T.-V. Nguyen, O.-B. Yang, Catal. Today 87 (2003) 69.
[35] T.-V. Nguyen, S. Kim, O.-B. Yang, Catal. Commun. 5 (2004) 59.
[36] D.R. Lide, Handbook of Chemistry and Physics, CRC Press, USA, 1994, pp. 12-91–12-95.
[37] K.W. Frese Jr., in: B.P. Sullivan, K. Krist, H.E. Guard (Eds.), Electrochemical and Electrocatalytic Reactions of Carbon Dioxide, Elsevier, Amsterdam, 1993, p. 191.
[38] Y. Hori, H. Wakebe, T. Tsukamoto, O. Koga, Surf. Sci. 335 (1995) 258.